Technical University of Denmark

DTU

Analytical and numerical modeling of front propagation and interaction of fronts in nonlinear thermoviscous

Rasmussen, Anders Rønne; Sørensen, Mads Peter; Gaididei, Yuri Borisovich; Christiansen, Peter Leth

DTU Library
Technical Information Center of Denmark

Analytical and numerical modeling of front propagation and interaction of fronts in nonlinear thermoviscous fluids including dissipation

Anders R. Rasmussen* and Mads P. Sørensen
Department of Mathematics, Technical University of Denmark, DK-2800 Kongens Lyngby, Denmark

Yuri B. Gaididei
Bogolyubov Institute for Theoretical Physics, 03680 Kiev, Ukraine

Peter L. Christiansen
*Department of Informatics and Mathematical Modelling and Department of Physics,
Technical University of Denmark, DK-2800 Kongens Lyngby, Denmark*
(Dated: June 3, 2008)

A wave equation, that governs finite amplitude acoustic disturbances in a thermoviscous Newtonian fluid, and includes nonlinear terms up to second order, is proposed. In contrast to the model known as the Kuznetsov equation, the proposed nonlinear wave equation preserves the Hamiltonian structure of the fundamental fluid dynamical equations in the non-dissipative limit. An exact traveling front solution is obtained from a generalized traveling wave assumption. This solution is, in an overall sense, equivalent to the Taylor shock solution of the Burgers equation. However, in contrast to the Burgers equation, the model equation considered here is capable to describe waves propagating in opposite directions. Owing to the Hamiltonian structure of the proposed model equation, the front solution is in agreement with the classical Rankine-Hugoniot relations. The exact front solution propagates at supersonic speed with respect to the fluid ahead of it, and subsonic speed with respect to the fluid behind it, similarly to the fluid dynamical shock. Linear stability analysis reveals that the front is stable when the acoustic pressure belongs to a critical interval, and is otherwise unstable. These results are verified numerically. Studies of head-on colliding fronts demonstrate that the front propagation speed changes upon collision.

I. INTRODUCTION

The "classical" equation of nonlinear acoustics [1], the so-called Kuznetsov equation [2], governs finite amplitude acoustic disturbances in a Newtonian, homogeneous, viscous, and heat conducting fluid. The model equation and its paraxial approximation, the Khokhlov-Zabolotskaya-Kuznetsov (KZK) equation [2, 3], are occasionally encountered within studies related to nonlinear wave propagation. See e.g. the recent works by Jordan [4] who presented the derivation and analysis of an exact traveling wave solution to the one-dimensional Kuznetsov equation, and by Jing and Cleveland [5] who described a three-dimensional numerical code that solves a generalization of the KZK equation, and the references cited in the introductory sections of those papers. Other recent works based on the Kuznetsov equation include: analysis of energy effects accompanying a strong sound disturbance [6], studies of generation of higher harmonics and dissipation based on a 3D finite element formulation [7], and studies of nonlinear wave motion in cylindrical coordinates [8]. The derivations of the Kuznetsov equation [2, 9, 10] and related model equations [11, 12, 13]

are based on the complete system of the equations of fluid dynamics. It has been demonstrated that this system of equations is of Hamiltonian structure in the non-dissipative limit [14]. However, in the non-dissipative limit, the Kuznetsov equation does not retain the Hamiltonian structure.

In this paper we propose a nonlinear wave equation, which, in the non-dissipative limit, preserves the Hamiltonian structure of the fundamental equations. Furthermore, we present the derivation and analysis of an exact traveling front solution, which applies equally well to the proposed nonlinear wave equation and the Kuznetsov equation. The derivation of the exact solution is based on a *generalized* traveling wave assumption, which leads to a wider class of exact solutions compared to the one reported by Jordan [4, 15]. Furthermore, the introduction of the generalized assumption is necessary in order to interpret the results of numerical simulations of head-on colliding fronts presented in this paper. In order to relate our results to the classical literature, we demonstrate that the exact front solution retains a number of properties of the fluid dynamical shock. The paper is structured as follows: The proposed equation and its Hamiltonian structure are discussed in Section II. Section III contains the derivation of our exact traveling front solution and analysis of its stability properties. In Section IV we demonstrate that the front is related the classical shock. Section V presents numerical investigations of the front,

---

*Electronic address: anders_r_r@yahoo.com

while Section VI contains our conclusions.

II. NONLINEAR WAVE EQUATIONS

Equations governing finite amplitude acoustic disturbances in a Newtonian, homogeneous, viscous and heat conducting fluid may be derived from the following four equations of fluid dynamics: *the equation of motion*

$$\rho\left(\frac{\partial \mathbf{u}}{\partial t} + (\mathbf{u}\cdot\boldsymbol{\nabla})\mathbf{u}\right)$$
$$= -\boldsymbol{\nabla}p + \eta\Delta\mathbf{u} + \left(\frac{\eta}{3} + \zeta\right)\boldsymbol{\nabla}(\boldsymbol{\nabla}\cdot\mathbf{u}), \quad (1)$$

the equation of continuity

$$\frac{\partial\rho}{\partial t} + \boldsymbol{\nabla}\cdot(\rho\mathbf{u}) = 0, \quad (2)$$

the heat transfer equation

$$\rho T\left(\frac{\partial s}{\partial t} + (\mathbf{u}\cdot\boldsymbol{\nabla})s\right) = \frac{\eta}{2}\left(\frac{\partial u_i}{\partial x_j} + \frac{\partial u_j}{\partial x_i} - \frac{2}{3}\delta_{ij}\frac{\partial u_k}{\partial x_k}\right)^2$$
$$+ \zeta(\boldsymbol{\nabla}\cdot\mathbf{u})^2 + \kappa\Delta T, \quad (3)$$

and *the equation of state*

$$p = p(\rho, s). \quad (4)$$

Here $\mathbf{x} = (x, y, z)$ are the spatial (Cartesian) coordinates and t denotes time. $\mathbf{u} = (u, q, w)$ is the fluid particle velocity, ρ is the density of the medium, p, s, and T are the thermodynamic variables pressure, entropy and temperature, respectively. η and ζ are the coefficients of shear and bulk viscosity, and κ is the heat conductivity coefficient. Δ is the Laplace operator.

To obtain a nonlinear wave equation all dependent variables except one are eliminated from the system (1)–(4), resulting in a nonlinear wave equation for that single variable [2, 9, 10, 11, 12, 13]. The deviations of ρ, p, s, and T from their equilibrium values, ρ_0, p_0, s_0, and T_0 are assumed to be small, as well as the fluid particle velocity, $|\mathbf{u}|$. The heat conductivity coefficient κ and the viscosities η and ζ are also treated as small quantities. In order to obtain a second order approximation, all equations are written retaining terms up to second order in the small quantities. It is assumed that the flow is rotation free, $\boldsymbol{\nabla}\times\mathbf{u} = 0$, thus

$$\mathbf{u} \equiv -\boldsymbol{\nabla}\psi, \quad (5)$$

where ψ is the velocity potential. Furthermore, it has become customary to use the following approximation for the equation of state [16]

$$p - p_0 = c_0^2\left(\rho - \rho_0\right) + \frac{c_0^2}{\rho_0}\frac{B/A}{2}\left(\rho - \rho_0\right)^2$$
$$+ \left(\frac{\partial p}{\partial s}\right)_{\rho, s=s_0}(s - s_0), \quad (6)$$

TABLE I: Values of c_0, B/A, and b for three different substances. The values for b are rough estimates obtained from Eq. (8) neglecting the influence of bulk viscosity and thermal losses.

Substance	c_0 (m s^{-1})	B/A	b (m^2 s^{-1})
Water	1483 (20℃)[a]	5.0 (20℃)[b]	1.3×10^{-6} (20℃)[c]
Air	343 (20℃)[a]	0.4 (20℃)[b,d]	21×10^{-6} (27℃)[c]
Soft tissue	1540[e]	9.6 (37℃)[b,f]	N/A

[a] Ref. 19
[b] Ref. 17
[c] Values for ρ_0 and η are obtained from Ref. 19.
[d] Diatomic gas
[e] Ref. 20
[f] Human breast fat

where B/A is the fluid nonlinearity parameter [17] and $c_0^2 \equiv (\partial p/\partial\rho)_{s,\rho=\rho_0}$ is the small-signal sound speed. Then, from Eqs. (1)–(6) we obtain the following nonlinear wave equation

$$\frac{\partial^2\psi}{\partial t^2} - c_0^2\Delta\psi = \frac{\partial\psi}{\partial t}\Delta\psi$$
$$+ \frac{\partial}{\partial t}\left(b\Delta\psi + (\boldsymbol{\nabla}\psi)^2 + \frac{B/A - 1}{2c_0^2}\left(\frac{\partial\psi}{\partial t}\right)^2\right), \quad (7)$$

where b is the diffusivity of sound [18]

$$b \equiv \frac{1}{\rho_0}\left\{\frac{4}{3}\eta + \zeta + \kappa\left(\frac{1}{C_V} - \frac{1}{C_p}\right)\right\}, \quad (8)$$

and C_V and C_p denote the heat capacities at constant volume and pressure, respectively. Typical values of the physical parameters c_0, B/A, and b are given in Table I. In the first order approximation, Eq. (7) reduces to

$$\frac{\partial^2\psi}{\partial t^2} = c_0^2\Delta\psi. \quad (9)$$

Introducing Eq. (9) in the first term on the right hand side of Eq. (7), the Kuznetsov equation [2]

$$\frac{\partial^2\psi}{\partial t^2} - c_0^2\Delta\psi = \frac{\partial}{\partial t}\left(b\Delta\psi + (\boldsymbol{\nabla}\psi)^2 + \frac{B/A}{2c_0^2}\left(\frac{\partial\psi}{\partial t}\right)^2\right), \quad (10)$$

is obtained.

In absence of dissipation, i.e. $\eta = \zeta = 0$, Eqs. (1) and (2) possess Hamiltonian structure [14]. This property is, however, *not* retained in Eq. (10) with $b = 0$, i.e. the non-dissipative limit of the Kuznetsov equation is not Hamiltonian. In contrast, Eq. (7) *does* retain the Hamiltonian structure in the non-dissipative limit. Accordingly, the equation may be derived from the Lagrangian density

$$\mathcal{L} = \frac{(\psi_t)^2}{2} - c_0^2\frac{(\boldsymbol{\nabla}\psi)^2}{2} - \frac{B/A - 1}{6c_0^2}(\psi_t)^3 - \frac{\psi_t(\boldsymbol{\nabla}\psi)^2}{2}, \quad (11)$$

using the Euler-Lagrange equation[1]. From the Legendre transformation [22] we obtain the corresponding Hamiltonian density as

$$\mathcal{H} = c_0^2 \frac{(\boldsymbol{\nabla}\psi)^2}{2} + \frac{(\psi_t)^2}{2} - \frac{B/A-1}{3c_0^2}(\psi_t)^3, \quad (12)$$

which may be integrated to yield the total Hamiltonian

$$H = \int_{-\infty}^{+\infty}\int_{-\infty}^{+\infty}\int_{-\infty}^{+\infty} \mathcal{H}\,dx\,dy\,dz. \quad (13)$$

Taking the time derivative of H in Eq. (13) with $\mathcal{H}$ replaced by Eq. (12), and using Eq. (7), one can obtain a simple expression for dH/dt. Doing this in one spatial dimension we obtain after some calculations

$$\frac{dH}{dt} = \left[c_0^2\psi_t\psi_x + (\psi_t)^2\,\psi_x\right]_{-\infty}^{+\infty} - b\int_{-\infty}^{+\infty}(\psi_{xt})^2\,dx. \quad (14)$$

In Eq. (14), which is sometimes called the energy balance equation, we observe that the first terms on the right hand side correspond to energy in- and output at the two boundaries, and that the last term accounts for energy dissipation inside the system.

In the remaining portion of this paper we shall limit the analysis to one-dimensional plane fields, in which case the proposed model equation (7) reduces to

$$\psi_{tt} - c_0^2\psi_{xx} = \psi_t\psi_{xx}$$
$$+ \frac{\partial}{\partial t}\left(b\psi_{xx} + (\psi_x)^2 + \frac{B/A-1}{2c_0^2}(\psi_t)^2\right), \quad (15)$$

where subscripts indicate partial differentiation.

Finally, for later reference we give the second-order expressions for the acoustic density, $\rho - \rho_0$, and acoustic pressure, $p - p_0$, in terms of the velocity potential, ψ. From the equations of motion (1) and state (6), subject to the basic assumptions of the derivation of the two model equations (7) and (10), we obtain

$$\rho - \rho_0 = \frac{\rho_0}{c_0^2}\left(\psi_t - \frac{(\psi_x)^2}{2} - \frac{B/A-1}{2c_0^2}(\psi_t)^2 - b\psi_{xx}\right), \quad (16)$$

and

$$p - p_0 = \rho_0\left(\psi_t - \frac{(\psi_x)^2}{2} + \frac{1}{2c_0^2}(\psi_t)^2\right) - \left(\frac{4}{3}\eta + \zeta\right)\psi_{xx}, \quad (17)$$

respectively. It should be noted that Eqs. (16) and (17) are derived from the fundamental equations, thus, the expressions are not specific to any of the two model equations (7) and (10).

III. EXACT TRAVELING FRONT SOLUTION

Recently, a standard traveling wave approach was applied to the one-dimensional approximation of the Kuznetsov equation (10) to reveal an exact traveling wave solution [4, 15]. In this section we extend the standard approach by introducing a generalized traveling wave assumption and analyze the stability properties of the solution.

A. Generalized traveling wave analysis

We introduce the following generalized traveling wave assumption

$$\psi(x,t) = \Psi(x - vt) - \lambda x + \sigma t$$
$$\equiv \Psi(\xi) - \lambda x + \sigma t, \quad (18)$$

where λ and σ are arbitrary constants, v denotes the wave propagation velocity, and $\xi \equiv x - vt$ is a wave variable. The inclusion of $-\lambda x + \sigma t$ in Eq. (18) leads to a wider class of exact solutions, compared to the one obtained from the assumption $\psi = \Psi(x - vt)$, which is the standard one. Furthermore, the introduction of the generalized assumption is necessary in order to interpret the results of numerical simulations of head-on colliding fronts presented in Section V B. Inserting Eq. (18) into the nonlinear wave equation (15) we obtain the ordinary differential equation

$$\left(v^2 - c_0^2\right)\Psi'' = \left(-v\Psi' + \sigma\right)\Psi'' - v\frac{d}{d\xi}\left\{b\Psi''\right.$$
$$\left. + (\Psi' - \lambda)^2 + \frac{B/A-1}{2c_0^2}\left(-v\Psi' + \sigma\right)^2\right\}, \quad (19)$$

where prime denotes ordinary differentiation with respect to ξ. Integrating once and introducing $\Phi \equiv -\Psi'$, Eq. (19) reduces to

$$C = vb\Phi' - \left(\frac{3}{2} + \frac{B/A-1}{2c_0^2}v^2\right)v\Phi^2 +$$
$$\left\{\left(1 - \frac{B/A-1}{c_0^2}\sigma\right)v^2 - 2\lambda v - c_0^2 - \sigma\right\}\Phi, \quad (20)$$

---

[1] Letting $\eta = \zeta = 0$, $\mathbf{u} = -\boldsymbol{\nabla}\psi$, and $p = \rho^\gamma/\gamma$ in Eqs. (1–2), and (4), respectively, one can derive the Lagrangian density

$$\mathcal{L}_{PEE} = \frac{c_0^4}{\gamma}\left(1 + \frac{\gamma-1}{c_0^2}\left(\psi_t - \frac{(\boldsymbol{\nabla}\psi)^2}{2}\right)\right)^{\frac{\gamma}{\gamma-1}},$$

corresponding to the potential Euler equation (PEE) given in Ref. 21. Expanding $\mathcal{L}_{PEE}$ to third order and letting $\gamma = B/A+1$ we obtain Eq. (11).

where C is a constant of integration. Requiring that the solution satisfy $\Phi' \to 0$ as $\xi \to \pm\infty$, and either

$$\Phi \to \begin{cases} \theta, & \xi \to +\infty \\ 0, & \xi \to -\infty \end{cases} \quad \text{or} \quad \Phi \to \begin{cases} 0, & \xi \to +\infty \\ \theta, & \xi \to -\infty \end{cases}, \quad (21)$$

where θ is an arbitrary constant, lead us to $C = 0$ and

$$\frac{B/A - 1}{2c_0^2} \theta v^3 - \left(1 - \frac{B/A - 1}{c_0^2}\sigma\right) v^2$$
$$+ \left(\frac{3}{2}\theta + 2\lambda\right) v + c_0^2 + \sigma = 0. \quad (22)$$

In order to obtain our traveling wave solution, we separate the variables in Eq. (20) subject to $C = 0$, then, using Eq. (22), we find the solution to be the traveling front

$$\Phi = \frac{\theta}{2}\left\{1 - \tanh\left(\frac{2(\xi - x_0)}{l}\right)\right\}, \quad (23)$$

$$l \equiv \frac{4b}{\left(\dfrac{B/A - 1}{2c_0^2}v^2 + \dfrac{3}{2}\right)\theta}, \quad (24)$$

where x_0 is an integration constant, $|l|$ is the front thickness, and $0 < \Phi < \theta$. Finally, using $\Phi = -\Psi'$ and inserting Eq. (23) into Eq. (18) we obtain (apart from an arbitrary constant of integration)

$$\psi(x,t) = -\frac{\theta}{2}\left\{\xi - \frac{l}{2}\ln\left(\cosh\frac{2(\xi - x_0)}{l}\right)\right\} - \lambda x + \sigma t, \quad (25)$$

which is the exact solution for the velocity potential.

Traveling tanh solutions, such as the front solution (23), are often called Taylor shocks. The existence of an exact solution of this type to the classical Burgers equation is a well known result [23]. However, the Burgers equation is restricted to wave propagation *either* to the left or to the right. The model equation considered in this paper does not suffer from this limitation, as shall be illustrated in Section V B.

Regarding the exact solution derived above, the physical properties of the flow associated with the traveling front are obtained from the partial derivatives of Eq. (25), which are given by

$$-\psi_x = \Phi + \lambda \quad \text{and} \quad \psi_t = v\Phi + \sigma. \quad (26)$$

According to Eq. (5) the fluid particle velocity is obtained as $u = -\psi_x$, and the first order approximation of Eq. (17) yields the acoustic pressure as $p - p_0 \approx \rho_0\psi_t$. The boundary conditions of the front are obtained from Eqs. (23) and (26) as

$$-\psi_x \to \begin{cases} \theta + \lambda, & \xi \to \mp\infty \\ \lambda, & \xi \to \pm\infty \end{cases}, \quad (27a)$$

$$\psi_t \to \begin{cases} v\theta + \sigma, & \xi \to \mp\infty \\ \sigma, & \xi \to \pm\infty \end{cases}, \quad (27b)$$

where upper (lower) signs apply for $l > 0$ ($l < 0$). Hence, the four parameters v, θ, λ, and σ, that was introduced in the derivation of the exact solution, determine the four boundary conditions of the front. From these boundary conditions we find that θ and $v\theta$ correspond to the heights of the jump across the front measured in $-\psi_x$ and ψ_t, respectively, see Fig. 1. At this point it is appropriate to emphasize that, in order for the exact solution to exist, the four parameters v, θ, λ, and σ must satisfy the cubic equation (22). Furthermore, the allowable values of the wave propagation velocity correspond to the *real* roots of this equation. A noticeably property of Eq. (22), which will prove useful later on, is that the equation is invariant under the transformation

$$v \to v, \quad \theta \to -\theta, \quad \lambda \to \theta + \lambda, \quad \sigma \to v\theta + \sigma. \quad (28)$$

Also the boundary conditions (27) are invariant, since, according to Eq. (24), the above transformation leads to $l \to -l$.
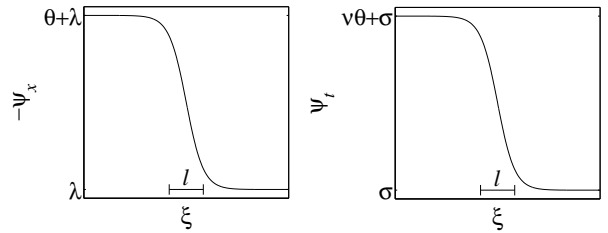

FIG. 1: The exact solution of Eq. (15) represents a traveling front. In order for the solution to exist, the wave propagation velocity, v, the front height, θ, and the two constants, λ and σ, must satisfy Eq. (22). The plot shows a front with $l > 0$.

In order to investigate the relationship between the front height, θ, and the front propagation velocity, v, we solve Eq. (22) with respect to θ to obtain

$$\theta = \frac{\left(1 - \dfrac{B/A - 1}{c_0^2}\sigma\right)v^2 - 2\lambda v - c_0^2 - \sigma}{v\left(\dfrac{3}{2} + \dfrac{B/A - 1}{2c_0^2}v^2\right)}. \quad (29)$$

For $B/A < 1$ the curve $\theta(v)$ has singularities at

$$v = v_s \equiv \pm\left(\frac{3c_0^2}{1 - B/A}\right)^{1/2}, \quad (30)$$

and for $B/A > 1$ the curve has a maximum[2] at $(v, \theta) = (v_{max}, \theta_{max})$, where v_{max} is obtained as

$$v_{max} = c_0\left(\frac{3\,B/A + \sqrt{9\,(B/A)^2 + 12(B/A - 1)}}{2(B/A - 1)}\right)^{1/2}, \quad (31)$$

———

[2] The critical point $(v, \theta) = (v_{max}, \theta_{max})$ was identified by Jordan [4] as the solution bifurcation point.

when $\lambda = 0$ and $\sigma = 0$. These two characteristic properties of the curve are illustrated in Fig. 2.
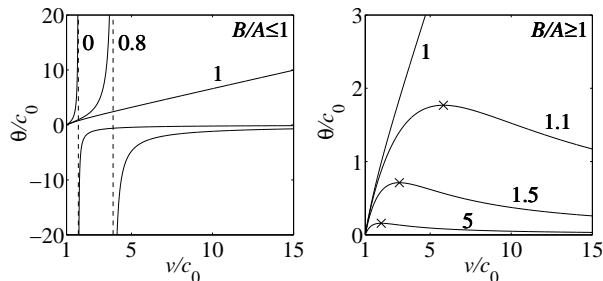

FIG. 2: The plots show the relationship between the front height, θ, and the front propagation velocity, v, given by Eq. (29) with $\lambda = 0$, $\sigma = 0$, and $B/A = \{0, 0.8, 1, 1.1, 1.5, 5\}$ (see labels on the plots). The dashed lines indicate the singularity at $v = v_{\mathrm{s}}$, which is defined in Eq. (30), and crosses indicate the maximum $(\theta, v) = (\theta_{\max}, v_{\max})$ defined in Eq. (31).

Finally, it should be emphasized that the generalized traveling wave analysis conducted above also applies to the one-dimensional approximation of the Kuznetsov equation (10). In this case Eq. (22) is replaced by[3]

$$\frac{B/A}{2c_0^2}\theta v^3 - \left(1 - \frac{B/A}{c_0^2}\sigma\right)v^2 + (\theta + 2\lambda)\, v + c_0^2 = 0, \quad (32)$$

and Eq. (24) by

$$l = \frac{4b}{\left(\dfrac{B/A}{2c_0^2}v^2 + 1\right)\theta}. \quad (33)$$

Apart from these changes, a generalized traveling wave analysis of the Kuznetsov equation is basically identical to that of Eq. (15).

The Hamiltonian structure, however, is unique to the proposed nonlinear wave equation (7) and its one-dimensional approximation Eq. (15). In order to establish a relationship between the exact solution, derived in this section, and the Hamiltonian structure of the governing equation, we insert Eq. (25) into Eq. (14) and the one-dimensional approximations of Eqs. (12) and (13). Then, after some calculations, we find that Eq. (14) reduces to the cubic equation (22). Hence, the exact traveling front solution of the proposed Hamiltonian model equation (15) satisfies the energy balance equation (14).

B. Linear stability analysis

In order to gain insight into the stability properties of the traveling front solution we initially consider the

---

[3] Eliminating λ and σ from Eq. (32) makes the equation equivalent to the previously reported result [4]

constant solution

$$-\psi_x = K \qquad \text{and} \qquad \psi_t = L, \quad (34)$$

which satisfies the nonlinear wave equation (15). The two constants K and L are arbitrary. In order to investigate the linear stability properties of this solution, we add small perturbation terms to the constant values as

$$-\psi_x = K - \varepsilon\chi_x \qquad \text{and} \qquad \psi_t = L + \varepsilon\chi_t, \quad (35)$$

where $\chi = \chi(x, t)$ and $\varepsilon \ll 1$. Then, inserting Eqs. (35) into Eq. (15) and keeping terms up to first order in ε we obtain the following linear perturbation equation

$$\left(1 - \frac{B/A - 1}{c_0^2}L\right)\chi_{tt} - \left(c_0^2 + L\right)\chi_{xx} = b\chi_{xxt} - 2K\chi_{xt}. \quad (36)$$

Inserting the single Fourier mode

$$\chi(x, t) = D\, e^{\mathrm{i}(kx - \omega t)}, \quad (37)$$

where D is the amplitude, k is the wave number, and ω is the angular frequency, into Eq. (36), we obtain the following dispersion relation

$$\left(\frac{B/A - 1}{c_0^2}L - 1\right)\omega^2 + \left(2Kk - \mathrm{i}bk^2\right)\omega + \left(c_0^2 + L\right)k^2 = 0. \quad (38)$$

The constant solution (34) is asymptotically stable only if all solutions of Eq. (36) approach zero as $t \to \infty$. This is the case when the imaginary part of both roots in Eq. (38), ω_1 and ω_2, are negative. It can be shown that for $B/A > 1$ the only requirement in order for the imaginary part of both roots to be negative is

$$-c_0^2 < L < \frac{c_0^2}{B/A - 1}. \quad (39)$$

When $B/A < 1$ the only requirement for both roots to have a negative imaginary part is

$$-c_0^2 < L < \infty. \quad (40)$$

Hence, the stability properties of the constant solution (34) are determined exclusively by L, i.e. the constant value of ψ_t. Recall that the acoustic pressure is proportional to ψ_t, thus, the level of the acoustic pressure determines the stability properties of the solution.

In order for the front solution to be stable, it is a necessary condition that both left and right asymptotic values of ψ_t, given by Eq. (27b), belong to the interval (39) when $B/A > 1$, and the interval (40) when $B/A < 1$. In Section V A we shall further investigate this stability criterion by means of numerical simulations.

IV. FRONT-SHOCK RELATIONSHIP

Within fluid dynamics, a shock denotes a sharp change of the physical quantities. A shock propagates at supersonic speed with respect to the fluid ahead of it, while it remains subsonic with respect to the fluid behind it. The physical quantities of the flow on each side of the shock are connected by the Rankine-Hugoniot relations, which are conservation equations for mass, momentum and energy. In the following we shall demonstrate that the front solution of the proposed Hamiltonian model equation (15) retains these properties.

A. The Rankine-Hugoniot relations

Using square brackets to denote the change in value of any quantity across a shock, e.g.

$$[\rho] = \rho_{\rm a} - \rho_{\rm b}, \qquad (41)$$

where b denotes the value behind the shock and a denotes the value ahead of it, the Rankine-Hugoniot relations may be written as [24]

$$\text{mass}: \quad [\rho(u-v)] = 0, \qquad (42)$$

$$\text{momentum}: \quad \left[p + \rho(u-v)^2\right] = 0, \qquad (43)$$

$$\text{energy}: \quad \left[h + (u-v)^2/2\right] = 0, \qquad (44)$$

where v is the shock propagation velocity and h is the enthalpy.

We now replace u, ρ, p, and h with expressions in terms of ψ_x and ψ_t, and write all equations retaining terms up to second order. Upon setting $u = -\psi_x$ and substituting Eqs. (16) and (17) into Eqs. (42) and (43) we thus obtain

$$\left[\left(\frac{(\psi_x)^2}{2} + \frac{B/A-1}{2c_0^2}(\psi_t)^2\right)v \right.$$
$$\left. - \psi_t(\psi_x + v) - c_0^2\psi_x\right] = 0, \quad (45)$$

and

$$\left[\frac{B/A-1}{2c_0^2}(\psi_t)^2 v^2 - \psi_t v^2 - 2\psi_t\psi_x v \right.$$
$$\left. - \frac{(\psi_t)^2}{2} - 2c_0^2\psi_x v - c_0^2\psi_t\right] = 0, \quad (46)$$

respectively. The dissipative terms involving κ, ζ, and η do not appear in Eqs. (45) and (46), since $\psi_{xx} \to 0$ ahead of and behind the front. The changes in ψ_x and ψ_t across the front are obtained from the boundary conditions (27). Assuming that $l > 0$ and $v > 0$, and using the notation introduced in Eq. (41) we may write

$$[\psi_x] = \theta, \qquad [\psi_t] = -v\theta. \qquad (47\text{a})$$

Furthermore, changes in products of ψ_x and ψ_t are

$$\left[(\psi_x)^2\right] = -\theta^2 - 2\theta\lambda, \qquad (47\text{b})$$

$$\left[(\psi_t)^2\right] = -v^2\theta^2 - 2v\theta\sigma, \qquad (47\text{c})$$

$$\left[\psi_x\psi_t\right] = v\theta^2 + v\theta\lambda + \theta\sigma. \qquad (47\text{d})$$

Inserting Eqs. (47) into Eqs. (45) and (46) *both* conservation equations reduce to the cubic equation (22). This striking result leads to the conclusion, that Eq. (22) implies conservation of mass and momentum. At this point it should be noted that the generalized traveling wave analysis of the Kuznetsov equation (10) leads to the cubic equation (32), which is *not* in agreement with the conservation equations for mass and momentum.

In order to handle the enthalpy in the condition for energy conservation (44) we shall make use of the following fundamental thermodynamic relationship [24]

$$\boldsymbol{\nabla}h = \frac{\boldsymbol{\nabla}p}{\rho}. \qquad (48)$$

Using the equation of motion (1), subject to the basic assumptions of the derivation of the model equations in Section II, we obtain from Eq. (44)

$$[\psi_t + v\psi_x] = 0. \qquad (49)$$

Alternatively, Eq. (49) follows directly from the generalized traveling wave assumption (18). Hence, the traveling wave assumption implies energy conservation in the flow.

B. Sub-/supersonic speeds of propagation

In order to determine whether the traveling front solution, derived in Section III A, propagates at sub- or supersonic speed with respect to the fluid ahead of it and the fluid behind it, we need to introduce the speed of sound in these regions of the fluid. Without loss of generality, we may consider only fronts propagating in the positive direction, $v > 0$, since Eq. (15) is invariant under the transformation $x \to -x$. Furthermore, we shall limit the analysis to stable fronts, i.e. ψ_t must belong to the interval (39) when $B/A > 1$, and the interval (40) when $B/A < 1$. Then, letting $\theta \to 0$ in Eq. (22) and solving for v yields the small signal propagation velocity, which is equivalent to the speed of sound, c. Introducing $\lambda = K$ and $\sigma = L$ we obtain

$$v = c(K,L) \equiv \frac{K + \sqrt{K^2 + (L+c_0^2)\left(1 - \frac{B/A-1}{c_0^2}L\right)}}{1 - \frac{B/A-1}{c_0^2}L},$$
$$(50)$$

where K and L denote the constant levels of $-\psi_x$ and ψ_t, respectively, at which the speed of sound (50) is evaluated. Inserting the boundary conditions of the front into

Eq. (50), i.e. substituting Eq. (27a) for K and Eq. (27b) for L, we obtain the speed of sound ahead of, c_{a}, and behind, c_{b}, the front

$$c_{\substack{\mathrm{a} \\ \mathrm{b}}} = c(\lambda, \sigma), \quad (51)$$

$$c_{\substack{\mathrm{b} \\ \mathrm{a}}} = c(\theta + \lambda, v\,\theta + \sigma), \quad (52)$$

where upper (lower) subscripts apply for $l > 0$ ($l < 0$). Note that, under the transformation (28), Eq. (52) transforms into Eq. (51). Hence, without loss of generality we shall consider only Eq. (51) in the following.

In order to compare the front propagation velocity, v, to c_{a} and c_{b} we make the following observations. Inserting Eq. (29) into Eq. (24) yields

$$l = \frac{4bv}{\left(1 - \dfrac{B/A - 1}{c_0^2}\sigma\right)v^2 - 2\lambda v - c_0^2 - \sigma}. \quad (53)$$

The denominator in Eq. (53) becomes zero when $v = c(\lambda, \sigma)$, where $c(\lambda, \sigma)$ is given by Eq. (50). Then, given that $v > 0$, we obtain from Eq. (53) that

$$v > c(\lambda, \sigma) \Leftrightarrow l > 0 \quad \text{and} \quad v < c(\lambda, \sigma) \Leftrightarrow l < 0. \quad (54)$$

Finally, from Eqs. (51) and (54) it follows that

$$v > c_{\mathrm{a}} \quad \text{and} \quad v < c_{\mathrm{b}}. \quad (55)$$

Hence, in all cases, the propagation velocity of the exact traveling front solution is supersonic with respect to the fluid ahead of the front, and subsonic with respect to the fluid behind it.

V. NUMERICAL RESULTS

All numerical calculations rely on a commercially available software package[4], which is based on the finite element method. For convenience we introduce the following non-dimensional variables, denoted by tilde

$$\tilde{\psi}(\tilde{x}, \tilde{t}) = \frac{1}{b}\psi(x, t), \qquad \tilde{x} = \frac{c_0}{b}x, \qquad \tilde{t} = \frac{c_0^2}{b}t. \quad (56)$$

Under this transformation we may write Eq. (15) as

$$\psi_{tt} - \psi_{xx} = \psi_t \psi_{xx}$$
$$+ \frac{\partial}{\partial t}\left(\psi_{xx} + (\psi_x)^2 + \frac{B/A - 1}{2}(\psi_t)^2\right), \quad (57)$$

where the tildes have been omitted. From a comparison of Eqs. (15) and (57), we find that the results of the previous sections subject to $b = 1$ and $c_0 = 1$ apply to

─────────

[4] COMSOL version 3.2a, `http://www.comsol.com` (2005)

Eq. (57). Non-dimensional versions of the parameters, v, θ, λ, and σ, also indicated by tilde, become

$$\tilde{\lambda} = \frac{\lambda}{c_0}, \qquad \tilde{\sigma} = \frac{\sigma}{c_0^2}, \qquad \tilde{\theta} = \frac{\theta}{c_0}, \qquad \tilde{v} = \frac{v}{c_0}. \quad (58)$$

In the following analysis we consider only the non-dimensional formulation of the problem. For notational simplicity we shall omit the tildes.

A. Investigation of the front stability criterion

In order to investigate, numerically, the stability properties of the front, we chose as initial condition for the numerical solution, the exact solution given by Eqs. (25) and (26), and choose v, θ, λ, σ, and B/A such that Eq. (22) is satisfied. For the sake of clarity, we shall limit the numerical investigations to the specific case of $\lambda = 0$, $\sigma = 0$, $v > 0$, and $l > 0$, which, according to Eq. (27), corresponds to fronts propagating to the right into an unperturbed fluid.

A first numerical simulation is presented in Fig. 3. Evidently, the numerical algorithm successfully integrates the initial condition forward in time. This finding indicates that, for the specific choice of parameters, $v = 1.4$, $\theta = 0.127$, and $B/A = 5$, the front exists and is stable. A second numerical simulation is presented in Fig. 4. This initial condition is given a larger velocity, $v = 1.7$, and a larger height, $\theta = 0.153$, while $B/A = 5$ remains unchanged compared to the first example. The parameters are chosen such that Eq. (22) remains satisfied. Apparently, the numerical algorithm fails when integrating the solution forward in time, which indicates that the front is unstable for the specific choice of parameters. Given that $\sigma = 0$ and $l > 0$, the left and right asymptotes of the front are given by $\psi_t = v\theta$ and $\psi_t = 0$, respectively, according to Eq. (27b). Clearly, the right value belongs to the interval (39), thus, it does not causes instability of the front. However, if the left value, $v\theta$, lies outside the interval (39), it causes instability of the front. Inserting the value of B/A from the two examples above into Eq. (39), we find that in the first and second example, $v\theta$ lies inside and outside the interval (39), respectively. Hence, the behavior observed in Figs. 3 and 4 agrees with the stability criterion introduced in Section III B.

A large number of numerical simulations have been performed in order to systematically investigate the stability properties of the front. Within each simulation the parameters in the initial condition are, again, chosen such that Eq. (22) is satisfied. The result of this investigation is presented in Fig. 5. Still, $\sigma = 0$ and $l > 0$, such that the left asymptotic value of the front is given by $\psi_t = v\theta$. For $B/A > 1$ the stability threshold curve in the $(B/A, v)$-plane is obtained when $v\theta$ equals the upper bound of the interval (39). Using Eq. (29) we obtain

$$v\theta = \frac{1}{B/A - 1} \Rightarrow v = \frac{\sqrt{(B/A - 1)(2\,B/A + 1)}}{B/A - 1}. \quad (59)$$

For $B/A < 1$, the stability threshold curve is given by Eq. (30), since $v\theta$ lies within (outside) the interval (40) when $v < v_s$ ($v > v_s$), according to Eq. (29). The two stability threshold curves are included in Fig. 5. The fine agreement between the numerical results and the stability threshold curves indicates that the stability criterion, introduced in Section III B, is both necessary *and* sufficient in order for the front solution to be stable.
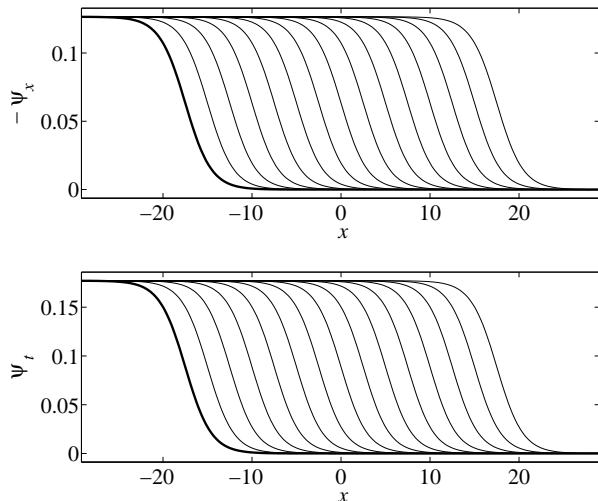

FIG. 3: The initial condition at $t = 0$ (bold line) is obtained from Eqs. (25) and (26) subject to $v = 1.4$, $\theta = 0.127$, $\lambda = 0$, $\sigma = 0$, and $B/A = 5$, which satisfy Eq. (22). The numerical solutions are shown over the time interval $0 \leq t \leq 25$.
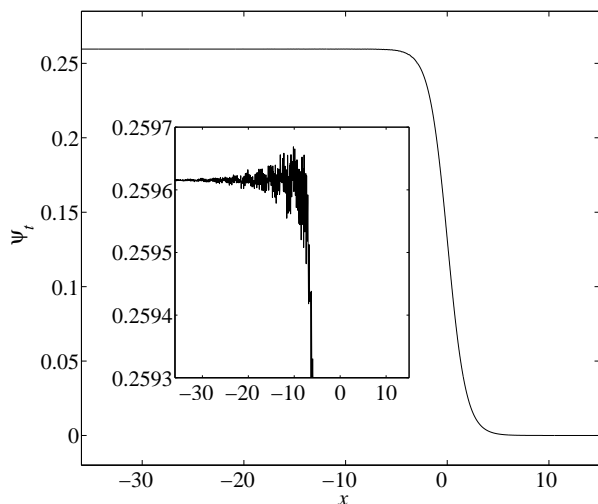

FIG. 4: The numerical algorithm fails to integrate this solution forward in time (insert shows magnification). See caption of Fig. 3. $v = 1.7$, $\theta = 0.153$, $\lambda = 0$, $\sigma = 0$, and $B/A = 5$. The numerical solution is shown at time $t = 3.8 \times 10^{-3}$.
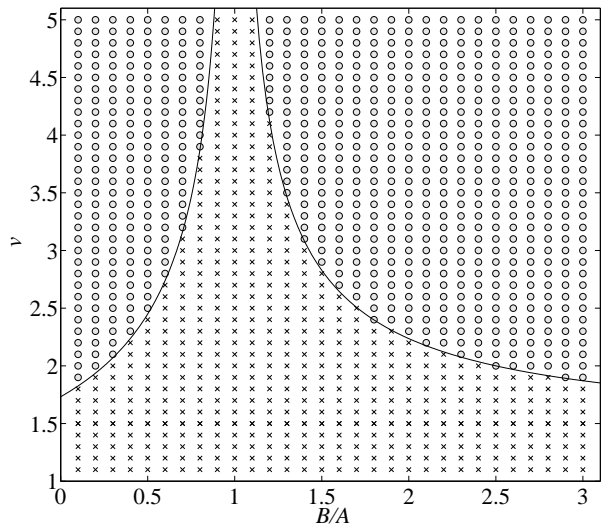

FIG. 5: Each point in the $(B/A, v)$-plane represents a numerical simulation, with the initial condition obtained from Eqs. (25) and (26) subject to $\lambda = 0$, $\sigma = 0$, and θ given by Eq. (29). Crosses and circles indicate stable and unstable solutions, respectively (compare with Figs. 3 and 4). Solid lines represent the stability threshold curves given by Eqs. (30) and (59).

B. Head-on colliding fronts

The numerical simulation presented in Fig. 6 shows the result of a head-on collision between two fronts. From the simulation we observe that two new fronts emerge upon the collision. The contour plot reveals that these fronts travel at a higher speed, compared to the speed of the fronts before the collision. For other choices of initial condition, we found the outcome of the head-on collision to be fronts traveling at lower speed, compared to that of the fronts before the collision.

In order to analyze solutions of Eq. (15) that comprise two fronts, we assume that these fronts belong to the class of exact front solutions derived in Section III A above. Investigations of the fronts that emerge upon a head-on collision have made it clear that this assumption is true, only when the generalized traveling wave assumption is considered, in contrast to the standard traveling wave assumption. Then, for each of the two fronts in the solution we introduce four new parameters, v, θ, λ, and σ, which must satisfy Eq. (22) as

$$\frac{B/A - 1}{2}\theta_i v_i^3 - (1 - (B/A - 1)\sigma_i)\, v_i^2$$
$$+ \left(\frac{3}{2}\theta_i + 2\lambda_i\right) v_i + \sigma_i + 1 = 0, \qquad i = 1, 2, \quad (60)$$

where subscript 1 and 2 denote parameters associated with waves positioned to the left and right, respectively. Furthermore, we require that solutions comprising two fronts are continuous and satisfy the following set of ar-

bitrary boundary conditions

$$-\psi_x \to \begin{cases} P, & x \to -\infty \\ Q, & x \to +\infty \end{cases}, \quad \psi_t \to \begin{cases} R, & x \to -\infty \\ S, & x \to +\infty \end{cases}.$$

(61)

Assuming that $l_1 > 0$ and $l_2 < 0$, we find, using Eq. (27), that the these requirements lead to the following conditions

$$\lambda_1 = \lambda_2 = P - \theta_1 = Q - \theta_2, \tag{62a}$$

$$\sigma_1 = \sigma_2 = R - v_1\theta_1 = S - v_2\theta_2, \tag{62b}$$

$$\theta_1 + \theta_2 = P - Q, \quad v_1\theta_1 + v_2\theta_2 = R - S. \tag{62c}$$

Then, we substitute the boundary values found in Fig. 6 for P, Q, R, and S in Eqs. (62), and substitute the value of B/A into Eq. (60). Finally, solving the system of equations (60) and (62), we obtain the results listed in Table II. The solution in the first row of the table corresponds to the initial fronts found in Fig. 6. The solution in the second row corresponds to two unstable fronts, according the stability criterion discussed above. The two fronts that emerge upon the head-on collision are defined by the values found in the third row of the table. Hence, the fronts after the collision travel at the velocities $-v_1 = v_2 = 1.76$, which is in agreement with the velocities determined from the slope of the contour lines in Fig. 6.

VI. CONCLUSIONS

A nonlinear wave equation that governs finite amplitude acoustic disturbances in a thermoviscous Newtonian fluid, and includes nonlinear terms up to second order, has been presented. The single dependent variable is the velocity potential. It has been demonstrated that, in the non-dissipative limit, the equation preserves the Hamiltonian structure of the fundamental fluid dynamical equations, hence, the model equation is associated with corresponding Lagrangian and Hamiltonian densities. Furthermore, we found that the Kuznetsov equation is an approximation of the proposed nonlinear wave equation. However, in the non-dissipative limit the Kuznetsov equation is not Hamiltonian. Exact traveling front solutions, for the partial derivatives with respect to space and time of the dependent variable, has been obtained using a generalized traveling wave assumption. This generalized assumption leads to a wider class of exact solutions compared the one obtained from a standard traveling wave assumption, since the generalized assumption includes two arbitrary constants, which are added to the partial derivatives. As a result of the generalized traveling wave analysis we found that, in order for the front to exist, its boundary values, its propagation velocity, and the physical parameters of the problem must satisfy a given cubic equation in the front propagation velocity. The derivation of the exact solution applies equally
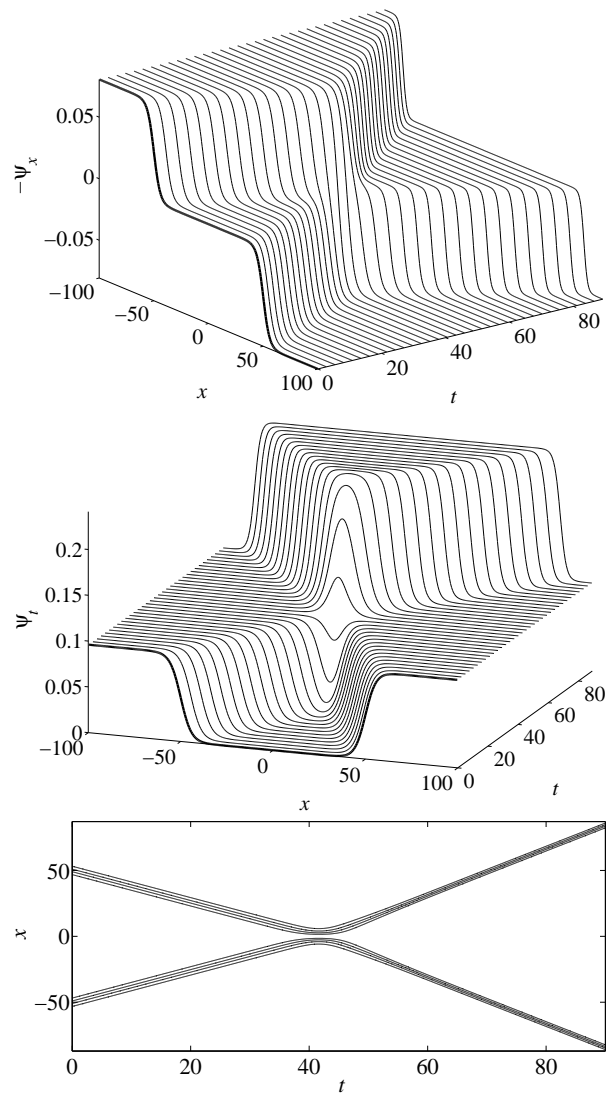

FIG. 6: The initial condition (bold lines in the two topmost plots), corresponds to two fronts that make a head-on collision at $t = 42$. The initial fronts are defined by $v_1 = -v_2 = 1.19$, $\theta_1 = -\theta_2 = 8.07 \times 10^{-2}$, $\lambda_1 = \lambda_2 = 0$, $\sigma_1 = \sigma_2 = 0$, and $B/A = 5$, where subscript 1 and 2 relate to fronts positioned the left and right, respectively. For each of the two fronts the parameters satisfy Eq. (22). Lowermost: contour lines given by $-\psi_x = Z$, where Z takes 4 equidistantly spaced values across each front.

well to the proposed Hamiltonian model equation and the Kuznetsov equation. Results for both equations have been given.

It has been demonstrated that the overall stability properties of the front are determined by the stability of the two asymptotic tails of the front. A linear stability analysis of these steady parts of the solution revealed that the front is stable when the partial derivative with respect to time, which is proportional to the acoustic pressure, belongs to a critical interval, and is otherwise unstable. This stability criterion has been verified numerically, by

TABLE II: Solution of Eqs. (60) and (62) subject to $P = -Q = 8.07 \times 10^{-2}$, $R = S = 9.60 \times 10^{-2}$, and $B/A = 5$ (compare with Fig. 6).

Solution	v_1	θ_1	v_2	θ_2	$\lambda_1 = \lambda_2$	$\sigma_1 = \sigma_2$
1	1.19	8.07×10^{-2}	-1.19	-8.07×10^{-2}	0	0
2	-3.25	8.07×10^{-2}	3.25	-8.07×10^{-2}	0	35.8×10^{-2}
3	-1.76	8.07×10^{-2}	1.76	-8.07×10^{-2}	0	23.8×10^{-2}

using the exact front solution as initial condition in a number of numerical simulations.

It has been demonstrated that, in all cases, the front propagates at supersonic speed with respect to the fluid ahead of it, while it remains subsonic with respect to the fluid behind it. The same properties have been reported for the classical fluid dynamical shock. Furthermore, it has been demonstrated that the cubic equation, mentioned above, is equivalent to the well established Rankine-Hugoniot relations, which connect the physical quantities on each side of a shock. However, this result was accomplished only when considering the cubic equation obtained from the analysis of the proposed Hamiltonian wave equation. The generalized traveling wave analysis based on the Kuznetsov equation is not in agreement with the Rankine-Hugoniot relations. Estimates of the front thickness may be obtained using the values for the diffusivity of sound listed in Table. I. In water and air front thicknesses are found to be of the order 10^{-9} and 10^{-7} meters, respectively. However, caution should be taken with these estimates, as the small length scales violates the continuum assumption of the governing equations.

Numerical simulations of two head-on colliding fronts have demonstrated that two new fronts emerge upon the collision, and that these fronts, in the general case, travel at speeds, which are different from the speeds of the fronts before the collision. It has been demonstrated that the velocities of the fronts after the collision may be calculated, based on information about the fronts before the collision. However, in order to accomplish this calculation, it has proven necessary to introduce the generalized traveling wave assumption in the derivation of the front solution.

In future studies, it would be rewarding to further investigate a variety of interacting fronts, other than the head-on collision reported in this paper. Also a search for other types of wave solutions, might learn us more about the properties of the proposed Hamiltonian model equation and the Kuznetsov equation.

Acknowledgments

[1] S. I. Aanonsen, T. Barkve, J. N. Tjøtta, and S. Tjøtta, "Distortion and harmonic generation in the nearfield of a finite amplitude sound beam", J. Acoust. Soc. Am. **75**, 749–768 (1984).

[2] V. P. Kuznetsov, "Equations of nonlinear acoustics", Sov. Phys. Acoust. **16**, 467–470 (1971).

[3] E. A. Zabolotskaya and R. V. Khokhlov, "Quasi-plane waves in the nonlinear acoustics of confined beams", Sov. Phys. Acoust. **15**, 35–40 (1969).

[4] P. M. Jordan, "An analytical study of Kuznetsov's equation: diffusive solitions, shock formation, and solution bifurcation", Phys. Lett. A **326**, 77–84 (2004).

[5] Y. Jing and R. O. Cleveland, "Modeling the propagation of nonlinear three-dimensional acoustic beams in inhomogeneous media", J. Acoust. Soc. Am. **122**, 1352–1364 (2007).

[6] J. Wójcik, "Conservation of energy and absorption in acoustic fields for linear and nonlinear propagation", J. Acoust. Soc. Am. **104**, 2654–2663 (1998).

[7] J. Hoffelner, H. Landes, M. Kaltenbacher, and R. Lerch, "Finite element simulation of nonlinear wave propagation in thermoviscous fluids including dissipation", IEEE Trans. Ultrason., Ferroelect., Freq. Contr. **48**, 779–786 (2001).

[8] A. Shermenev, "Separation of variables for the nonlinear wave equation in cylindrical coordinates", Physica D **212**, 205–215 (2005).

[9] B. O. Enflo and C. M. Hedberg, *Theory of Nonlinear Acoustics in Fluids* (Kluwer Academic, Dordrecht) (2002).

[10] S. Makarov and M. Ochmann, "Nonlinear and thermoviscous phenomena in acoustics, part II", Acustica **83**, 197–222 (1996).

[11] M. V. Aver'yanov, V. A. Khokhlova, O. A. Sapozhnikov, P. Blanc-Benon, and R. O. Cleveland, "Parabolic equation for nonlinear acoustic wave propagation in inhomogeneous moving media", Acoust. Phys. **52**, 623–632 (2006).

[12] K. Naugolnykh and L. Ostrovsky, *Nonlinear Wave Processes in Acoustics* (Cambridge University Press, Cambridge) (1998).

[13] L. H. Söderholm, "A higer order acoustic equation for the slightly viscous case", Acustica **87**, 29–33 (2001).

[14] V. E. Zakharov and E. A. Kuznetsov, "Hamiltonian formalism for nonlinear waves", Physics-Uspekhi **40**, 1087–1116 (1997).

[15] P. M. Jordan, "Bifurcations of diffusive soliton solutions to Kuznetsov's equation", J. Acoust. Soc. Am. **113**, 2283–2283 (2003).

[16] S. Makarov and M. Ochmann, "Nonlinear and thermoviscous phenomena in acoustics, part I", Acustica **82**, 579–606 (1996).

[17] R. T. Beyer, "The parameter B/A", in *Nonlinear Acoustics*, edited by M. F. Hamilton and D. T. Blackstock, chapter 2, 25–39 (Academic Press, San Diego) (1998).

[18] M. F. Hamilton and C. L. Morfey, "Model equations", in *Nonlinear Acoustics*, edited by M. F. Hamilton and D. T. Blackstock, chapter 3, 41–64 (Academic Press, San Diego) (1998).

[19] D. R. Lide, ed., *CRC Handbook of Chemistry and Physics, Internet Version 2007, (87th Edition), `http://www.hbcpnetbase.com`* (Taylor and Francis, Boca Raton) (2007).

[20] R. Gent, *Applied Physics and Technology of Diagnostic Ultrasound* (Milner Publishing, Prospect) (1997).

[21] I. Christov, C. I. Christov, and P. M. Jordan, "Modeling weakly nonlinear acoustic wave propagation", Q. J. Mechanics. Appl. Math. **60**, 473–495 (2007).

[22] H. Goldstein, C. Poole, and J. Safko, *Classical Mechanics*, 3 edition (Addison Wesley) (2001).

[23] M. F. Hamilton, D. T. Blackstock, and A. D. Pierce, "Progressive waves in lossless and lossy fluids", in *Nonlinear Acoustics*, edited by M. F. Hamilton and D. T. Blackstock, chapter 3, 65–150 (Academic Press, San Diego) (1998).

[24] L. D. Landau and E. M. Lifshitz, *Fluid mechanics* (Pergamon, Oxford) (1987).